

# Structure Selectivity of Alkaline Periodate Oxidation on Lignocellulose for Facile Isolation of Cellulose Nanocrystals

Peiwen Liu, Bo Pang, Sebastian Dechert, Xizhou Cecily Zhang, Loren B Andreas, Steffen Fischer, Franc Meyer, and Kai Zhang\*

**Abstract:** Reported here for the first time is the alkaline periodate oxidation of lignocelluloses for the selective isolation of cellulose nanocrystals (CNCs). With the high concentrations as a potassium salt at pH 10, periodate ions predominantly exist as dimeric orthoperiodate ions ( $H_2I_2O_{10}^{4-}$ ). With reduced oxidizing activity in alkaline solutions, dimeric orthoperiodate ions preferentially oxidized non-ordered cellulose regions. The alkaline surroundings promoted the degradation of these oxidized cellulose chains by  $\beta$ -alkoxy fragmentation and generated CNCs. The obtained CNCs were uniform in size and generally contained carboxy groups. Furthermore, the reaction solution could be reused after regeneration of the periodate with ozone gas. This method allows direct production of CNCs from diverse sources, in particular lignocellulosic raw materials including sawdust (European beech and Scots pine), flax, and kenaf, in addition to microcrystalline cellulose and pulp.

## Introduction

Periodate can selectively cleave carbon–carbon bonds of a variety of 1,2-difunctionalized alkanes, which makes it intriguing for a variety of fundamental and industrial applications, such as for functionalization of C–H bonds,<sup>[1]</sup> and either structure determination or derivatization in carbohydrate chemistry.<sup>[2]</sup> Periodate oxidation of polysaccha-

rides under relatively mild reaction conditions is widely used to endow the polysaccharide chains with aldehyde groups, for example, to transform cellulose into polymeric 2,3-dialdehyde cellulose.<sup>[2a,b,3]</sup> Usually, periodate oxidation is performed in mildly acidic solutions, whereas the periodate oxidation of lignocelluloses in alkaline solutions has not been reported. Inspired by our previous work,<sup>[4]</sup> the rarely used alkaline periodate oxidation shows potential in preparing cellulose nanocrystals (CNCs), which are recognized as a promising nanomaterial for future applications.<sup>[5]</sup>

It is well known that CNCs represent the highly ordered portions within cellulose and they have advantageous properties,<sup>[6]</sup> which include excellent mechanical properties, amphiphilicity, chirality, and variable surface chemistry. As a renewable bio-nanomaterial, CNCs are attracting and will continuously draw attention from academic and industrial fields.<sup>[7]</sup> However, native cellulose microfibrils generally contain both ordered and non-ordered regions, so the removal of non-ordered parts is necessary to obtain homogeneous CNCs. The existing methods for the separation of CNCs generally rely on the harsh degradation or separation of non-ordered parts using a strictly controlled process. This separation can generally be realized by cleaving the glycosidic bonds with corrosive mineral acids at high temperature,<sup>[8]</sup> by TEMPO-mediated oxidation of primary hydroxy groups,<sup>[9]</sup> by exploiting their different dissolution processes in ionic liquids,<sup>[10]</sup> or by the unselective acidic periodate oxidation of hydroxy groups at C2 and C3.<sup>[11]</sup> However, new selective chemical methods are still needed to significantly reduce the cost of producing CNCs, to further advance the applications of CNCs in our real life.

Herein, we show the selective, facile, and highly efficient isolation of CNCs by alkaline periodate oxidation (PO-CNCs) at pH 10 by preferentially oxidizing and degrading the non-ordered regions. This selective isolation is based on the structural difference between the ordered and non-ordered cellulose regions, which show different cyclization abilities with dimeric orthoperiodate ions. Salient features of our findings include: 1) the first alkaline periodate oxidation on diverse lignocelluloses, 2) a novel method for producing CNCs, 3) the first process combining periodate oxidation and  $\beta$ -alkoxy fragmentation in a one-pot reaction, 4) revealing the selectivity of alkaline periodate oxidation on cellulose having different structures, ordered and non-ordered, 5) mechanistic insights into selective alkaline periodate oxidation for the isolation of CNCs, and 6) confirmation of the existence of dimeric orthoperiodate ions ( $H_2I_2O_{10}^{4-}$ ).

[\*] P. Liu, B. Pang, Prof. Dr. K. Zhang  
Wood Technology and Wood Chemistry  
Georg-August-University of Göttingen  
37077 Göttingen (Germany)  
E-mail: kai.zhang@uni-goettingen.de

Dr. S. Dechert, Prof. Dr. F. Meyer  
Institute of Inorganic Chemistry, Georg-August-University of Göttingen, 37077 Göttingen (Germany)

X. C. Zhang, Dr. L. B. Andreas  
NMR-based Structural Biology, Max-Planck-Institute for Biophysical Chemistry, 37077 Göttingen (Germany)

Prof. Dr. S. Fischer  
Institute of Wood and Plant Chemistry, Dresden University of Technology, 01307 Tharandt (Germany)

Supporting information and the ORCID identification number(s) for the author(s) of this article can be found under:  
<https://doi.org/10.1002/anie.201912053>.

© 2019 The Authors. Published by Wiley-VCH Verlag GmbH & Co. KGaA. This is an open access article under the terms of the Creative Commons Attribution Non-Commercial License, which permits use, distribution and reproduction in any medium, provided the original work is properly cited, and is not used for commercial purposes.



## Results and Discussion

The periodate oxidation at pH 10 was performed firstly on microcrystalline cellulose (MCC), which can be taken as the pure cellulose (Figure 1). The effects of a few critical reaction parameters (pH value, the amount of periodate, reaction time, and temperature) were investigated (see Figure S2 in the Supporting Information). As the most suitable reaction conditions, 7.04 g (0.031 mol) of periodic acid ( $H_5IO_6$ ) were used to oxidize 1 g of MCC (0.0062 mol of anhydroglucose units) at room temperature for 14 days in the dark. The pH value was adjusted to  $10 \pm 0.05$  with an aqueous KOH solution at the beginning of the reaction (Figure 1 A and B). The total solids after the reaction were obtained by ultracentrifugation before purification with dialysis and the ultrasonication (180 W for 1 hour). After the removal of large fractions from purified total solids by the centrifugation at 3000 rpm at 25 °C for 20 minutes, PO-CNCs were obtained within the stable suspension as the supernatant. The contents of obtained PO-CNCs reached 40.1 wt. % after the collection of all possible CNCs from the total solids (see Table S1). The contents of the PO-CNCs after the first separation by ultracentrifugation were referred to as the minimal yields, and only the amount of the PO-CNCs from the first separation were used for the calculation of yield.

TEM and AFM images of the dried PO-CNCs revealed their typical needle-like morphology (Figure 1 C; see Figure S3). The PO-CNCs had a crystallinity of 57.1 % according to solid-state NMR analysis (see Figure S4). The surface zeta-

potential of the PO-CNCs was measured to be  $-25.5 \pm 5.0$  mV (see Figure S5). The PO-CNCs showed characteristic chiral nematic structures when dispersed in aqueous suspensions (Figure 1 D and S1). Successful preparation of PO-CNCs by alkaline periodate oxidation at pH 10 indicates efficient cleavage of the non-ordered regions within the cellulose microfibrils that represent the connections between the ordered domains. The reaction is highly efficient, as the ultrasonication treatment only increased the yield of the PO-CNCs by about 7 wt.%. In contrast, no CNCs were obtained in control experiments without periodate at the same pH value.

Similar to acidic periodate oxidation, the alkaline periodate oxidation starts with the cyclization of periodate ions and the dihydroxy groups at C2/C3 of the anhydroglucose units of cellulose. The cyclization between periodate ions and dihydroxy groups subject to general acid-base catalysis, which requires activated hydroxy groups either on C2 or C3.<sup>[12]</sup> It should be noted that the C3-hydroxy groups of cellulose chains in the outermost layers of the ordered domains are generally blocked by forming robust inter- and intramolecular hydrogen bonds for the ordered arrangement.<sup>[13]</sup> During the alkaline periodate oxidation, the activation of the deeply buried protons on the C3-hydroxy groups will need to overcome the steric hindrance and break the hydrogen bonds as well as Van der Waals forces. However, this process is strongly retarded because the increase of pH value from 4 to 10 decreases the oxidation potential ( $E_{Ox}$ ) of the periodate-iodate couple from  $-1.6$  V to  $-0.7$  V.<sup>[14]</sup> Therefore, the cyclization between dihydroxy groups in ordered regions

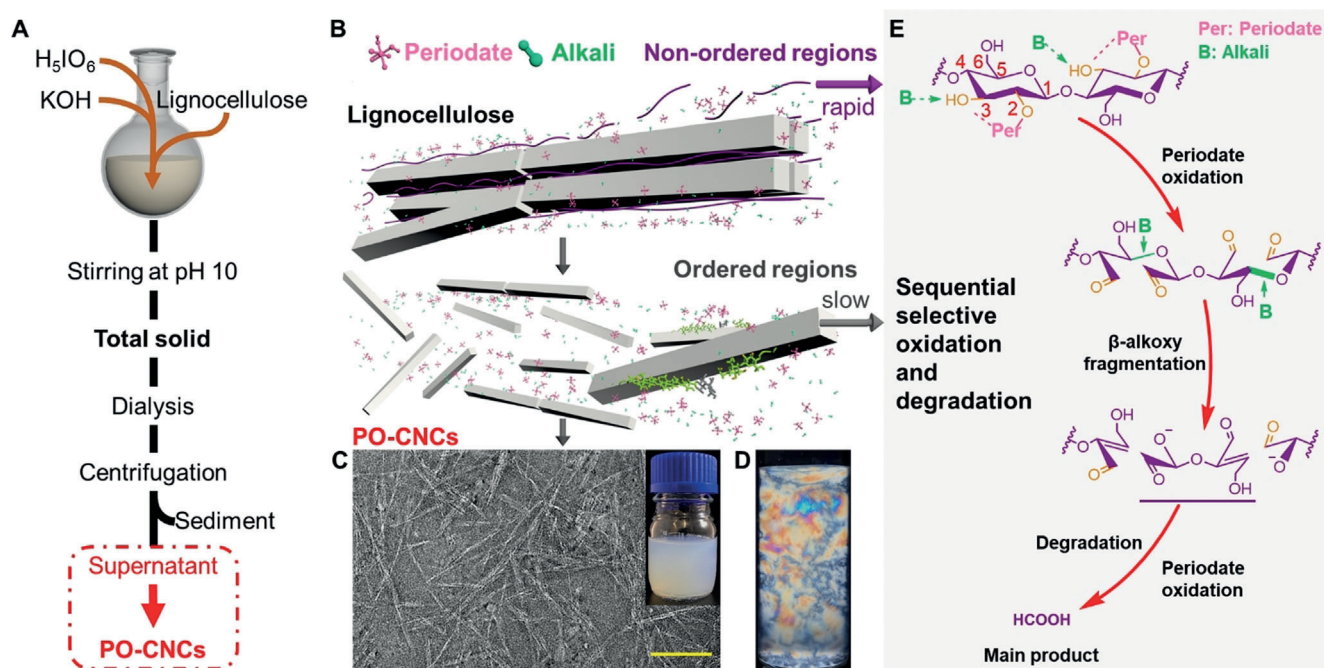


**Figure 1.** Selective separation of PO-CNCs by performing periodate oxidation at pH 10. A) Flow diagram representing the isolation process. B) Schematic representation of the isolation process on lignocellulose. (Simplified cartoons for the distribution of ordered and non-ordered regions within cellulose microfibrils are shown in the image for better visualization. The non-ordered regions are shown as chains along the elementary fibrils and single lines between ordered regions.). C) TEM image of PO-CNCs with the scale bar of 250 nm. The inset shows a photo of an aqueous PO-CNCs suspension (1 wt. %). D) Optical image of aqueous PO-CNCs suspension (1 wt. %) between crossed polarizers showing chiral nematic structures (see Figure S1). E) Proposed route for the selective oxidation of cellulose and further degradation, which results in soluble compounds.



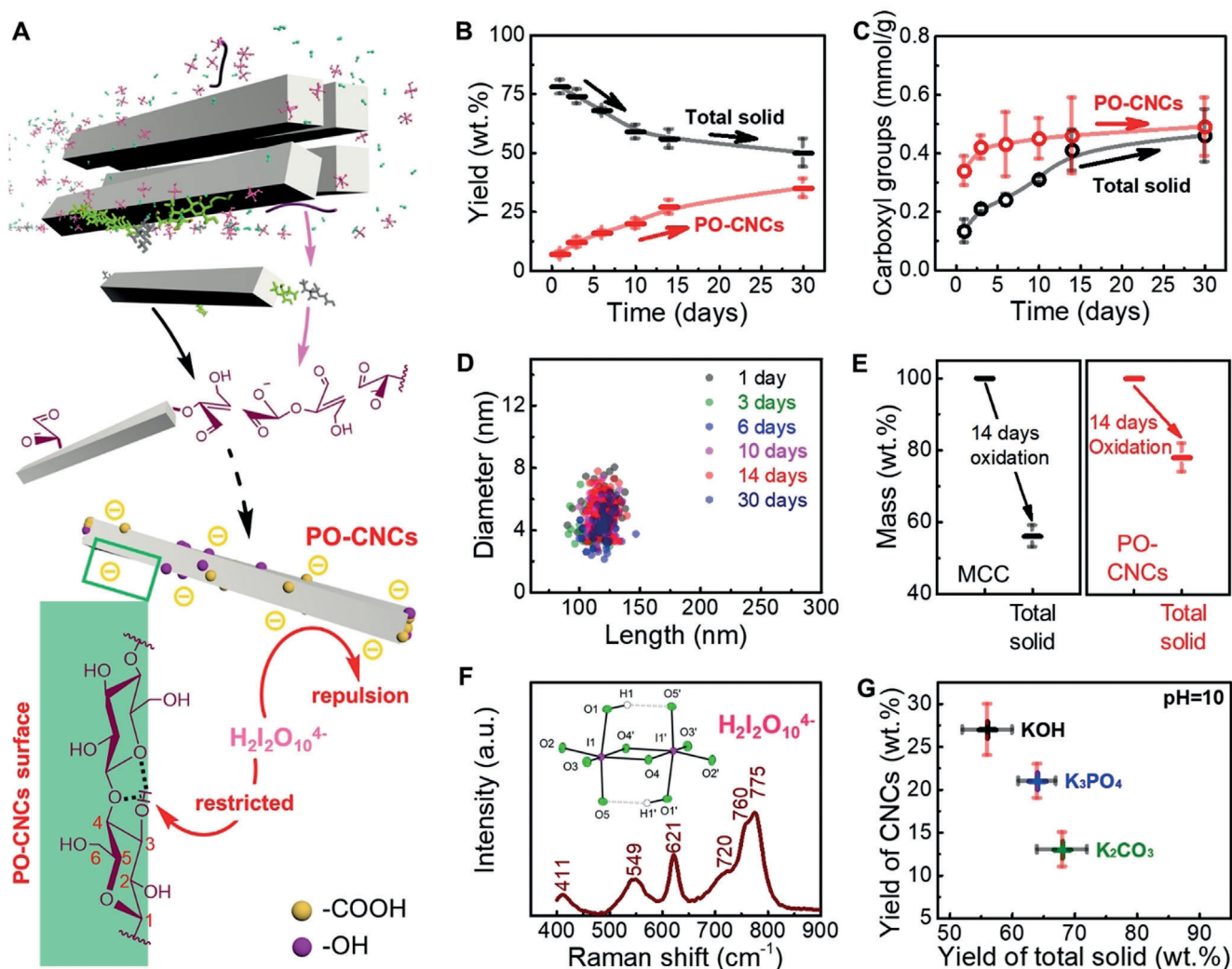


**Figure 2.** Selective isolation process for PO-CNCs. A) Schematic representation of the selective reaction leading to PO-CNCs with carboxy groups. B) Yields of recovered total solid and minimal yields of PO-CNCs after the reactions of up to 30 days. C) Average amounts of carboxy groups on recovered total solid and PO-CNCs. D) Size distributions of obtained PO-CNCs after the reaction of various days. E) Diverse mass reduction after 14 days periodate oxidation of MCC and PO-CNCs. F) A representative Raman spectrum of the reaction solution at pH 10 without MCC, showing dimeric orthoperiodate as the main form of periodate. G) The yields of the total solid and PO-CNCs after the periodate oxidation using diverse bases for adjusting pH value to 10.

and periodate ions is highly hampered in alkaline conditions (Figure 2A). In comparison, the C3-hydroxy groups within non-ordered regions should be readily accessible for the cyclization. Thus, periodate oxidation rates of ordered and non-ordered cellulose regions should be different, promoting the degradation of non-ordered regions and the isolation of PO-CNCs. Furthermore, the deprotonation of monoanionic periodate ( $\text{H}_4\text{IO}_6^-$ ) by hydroxide ions leads to dianionic periodate ( $\text{H}_3\text{IO}_6^{2-}$ ) or dimeric orthoperiodate ( $\text{H}_2\text{I}_2\text{O}_{10}^{4-}$ ) with more negative charges (see Figure S6). This arrangement enhances the electrostatic repulsion between periodate ions and the surface of the PO-CNCs (Figure 2A), further reducing the potential of cyclization between periodate ions and dihydroxy groups on the PO-CNC surface.

Despite the amplified difference in oxidation rates for ordered and non-ordered regions, around 44 wt.% of the cellulose is soluble in aqueous solution after 14 days of

reaction. The main product in solution was formic acid according to NMR analysis (see Figure S7). Based on previous reports about periodate oxidation of cellulose<sup>[14,15]</sup> and further degradation of oxidized cellulose,<sup>[16]</sup> a sequential selective oxidation and degradation route should be the primary procedure leading to soluble products (Figure 1E). The periodate oxidation slowly generates 2,3-dialdehyde cellulose at first,<sup>[15]</sup> which then undergoes rapid  $\beta$ -alkoxy fragmentation at the C5–O5 bonds.<sup>[16,17]</sup> The non-ordered regions are further oxidized, degraded, and removed from the bulk cellulose as water-soluble small molecules, and promote the release of PO-CNCs (Figure 1B). Thus, the alkaline periodate oxidation of cellulose at pH 10 demonstrates a highly selective oxidation and degradation process of non-ordered regions. The cleavage of both C2–C3 and C5–O5 bonds by periodate oxidation and  $\beta$ -alkoxy fragmentation demonstrates a novel strategy for yielding homogeneous PO-



CNCs. At the same time, rapid  $\beta$ -alkoxy fragmentation and further oxidation leads to carboxy groups on the PO-CNC surface instead of aldehyde groups (Figure 2A; see Figure S7).

The periodate oxidation was monitored for up to 30 days to investigate the details of this process (Figure 2A). The amount of total solids recovered from the isolation process decreased steadily with longer reaction times, while the minimal yield of PO-CNCs increased (Figure 2B). The yield of total solids from the original MCC was  $78 \pm 3$  wt. % after 24 hours,  $74 \pm 3$  wt. % after 3 days,  $68 \pm 1$  wt. % for 6 days,  $59 \pm 3$  wt. % for 10 days,  $56 \pm 4$  wt. % after 14 days, and  $50 \pm 6$  wt. % after 30 days. At the same time, the PO-CNCs with a minimal yield of  $7 \pm 1$  wt. % were obtained even after one day of reaction. The minimal yield of the PO-CNCs increased to  $12 \pm 2$  wt. %,  $16 \pm 1$  wt. % and  $20 \pm 2$  wt. % after reaction for 3, 6, and 10 days, respectively. After 14 days, PO-CNCs with a minimal yield of  $27 \pm 3$  wt. % were obtained and  $35 \pm 4$  wt. % of the PO-CNCs were harvested after 30 days of reaction.

It is obvious that the most rapid reduction of solid content happened within the first 24 hours and nearly 22 wt. % of cellulose was converted into soluble products. After that, the formation of soluble compounds became much slower. This observation could be attributed to the fast oxidation and degradation of non-ordered cellulose parts by the high concentration of periodate at the beginning. With the removal of most non-ordered regions, the ordered regions were partially modified and cleaved with time. Because of the consumption of periodate and the hampered reaction on the remained ordered parts of cellulose, the formation of soluble compounds became even slower after 10 days. Moreover, the isolation efficiency was reduced after 14 days of reaction. With the prolonged oxidation of up to 30 days, the total yield of the PO-CNCs was 42.7 wt. %. Only 2.6 wt. % of the PO-CNCs was produced in the following 16 days. In comparison, the increase of the total yield of the PO-CNCs was as much as 13.4 wt. % with a prolonged reaction from 10 to 14 days. Therefore, we selected 14 days as the optimal reaction time for this study (see Table S1).

Different than the aldehyde groups introduced after a general periodate oxidation in acidic surroundings, only carboxy groups were obtained in both the total solids and on the surface of the PO-CNCs (Figure 2A; see Figure S8). After 24 hours of reaction,  $0.13 \pm 0.04$  mmol g<sup>-1</sup> of the carboxy groups were detected in the total solids by using conductivity titration. The average concentrations of the carboxy groups in the total solids increased to  $0.21 \pm 0.01$ ,  $0.24 \pm 0.02$ ,  $0.31 \pm 0.01$ , and  $0.41 \pm 0.07$  mmol g<sup>-1</sup> after 3, 6, 10, and 14 day reactions, respectively. With the prolonged oxidation to 30 days, the concentration of the carboxy groups reached  $0.46 \pm 0.09$  mmol g<sup>-1</sup>. In comparison,  $0.34 \pm 0.04$  mmol g<sup>-1</sup> of the carboxy groups were found on the surface of the PO-CNCs even after 1 day reaction. The content of the carboxy groups increased slightly to  $0.42 \pm 0.04$ ,  $0.43 \pm 0.11$ , and  $0.45 \pm 0.07$  mmol g<sup>-1</sup> after 3, 6, and 10 day reactions, respectively. After 14 and 30 day reactions, the content of the carboxy groups was maintained at  $0.46 \pm 0.13$  and  $0.49 \pm 0.1$  mmol g<sup>-1</sup>, respectively (Figure 2C).

It is obvious that the content of the carboxy groups increased by  $0.15$  mmol g<sup>-1</sup> in total solids from 10 days to 30 days. In comparison, the content of the carboxy groups on the PO-CNCs surface was maintained after 3 days of reaction, and only slightly increased over longer reaction times of up to 30 days. Moreover, during the prolonged reaction from 10 to 30 days, only around 9 wt. % of the total solids was removed, but an additional 15 wt. % of the PO-CNCs was obtained (Figure 2B; see Table S1). Thus, PO-CNCs should have been isolated from the total solids during the oxidation at longer reaction times. The separation of PO-CNCs should predominantly result from the introduction of more carboxy groups in the ordered regions and preferentially on the surface of PO-CNCs, so that only little degradation and loss of total solids is observed. The separation process was slow, and is ascribed to the slow alkaline periodate oxidation on the surface of the PO-CNCs, as discussed above (Figure 2A). Furthermore, the highest content of the carboxy groups that could be introduced onto the PO-CNCs lay at nearly  $0.5$  mmol g<sup>-1</sup> by using this method.

Moreover, the dimensions of the PO-CNCs from MCC are distributed within a narrow range, independent of the reaction time (Figure 2D). The average diameters lie between  $3.7 \pm 1.9$  and  $5.3 \pm 2.4$  nm, and the average lengths are between  $116 \pm 18.9$  and  $120.1 \pm 17.3$  nm (see Table S2). These constant size distributions of the PO-CNCs indicate that the alkaline periodate oxidation at pH 10 prefers to remove the readily hydrolyzable regions down to the smallest possible dimension of the PO-CNCs. Further oxidation is impeded and becomes very slow as discussed above. This fact was further verified during an experiment by directly oxidizing PO-CNCs, isolated from a 14 day oxidation, under identical reaction conditions as used of the alkaline periodate oxidation on MCC at pH 10. Compared to the 14 day periodate oxidation on MCC with less specific surface area and a weight loss of around 44 wt. %, PO-CNCs underwent a weight loss of only about 20 wt. % after another 14 days of oxidation (Figure 2E). The morphology of the oxidized PO-CNCs and their size distributions were almost identical to the original PO-CNCs according to TEM measurements (see Figure S9). It should be noted that 0.031 mol of periodate was used to oxidize 0.0062 mol of the anhydroglucose units of the PO-CNCs. This amount of periodate is theoretically sufficient to oxidize all dihydroxy groups in the anhydroglucose units and convert all products from the  $\beta$ -alkoxy fragmentation into soluble compounds (Figure 1E). Thus, the alkaline periodate oxidation on ordered regions at pH 10 is hampered, while non-ordered cellulose regions are selectively modified and removed, leaving the ordered parts as PO-CNCs behind. Compared with the selective periodate oxidation, producing CNCs by acidic periodate oxidation (pH  $\approx$  4) was realized by reducing the amount of sodium periodate and the reaction time with the application of complicated post treatments.<sup>[11a,18]</sup> Moreover, periodate oxidation under acidic conditions is often used on either raw lignocelluloses or on nanocellulose as the pre- and post-treatment to either improve the separation or to introduce the carboxy/hydroxy groups.<sup>[11a,18,19]</sup> However, prior to this work, the selectivity of periodate oxidation for ordered and non-ordered cellulose



regions has not been reported, and is predominantly because of the low solubility of sodium salts of periodate under basic conditions.<sup>[14]</sup>

In addition to structural differences between non-ordered and ordered cellulose regions having distinct activities towards oxidation, the periodate speciation is the other critical parameter as we discussed above. It is well known that periodate is present as the monoanionic periodate ( $\text{H}_4\text{IO}_6^-$ ) in aqueous solution at pH 4 (see Figure S10). Periodate oxidation on MCC at pH 4 for 3 days generally results in 2,3-dialdehyde cellulose, instead of CNCs (see Figures S10 and S11).<sup>[20]</sup> In comparison, periodate is present as dimeric orthoperiodate ( $\text{H}_2\text{I}_2\text{O}_{10}^{4-}$ ) in aqueous solution at pH 10 based on the peaks at 411, 549, 621, 720, and 760  $\text{cm}^{-1}$  in the Raman spectrum (Figure 2F).<sup>[21]</sup> This dimer was also supported by X-ray crystallographic analysis of the crystals of  $\text{K}_4\text{H}_2\text{I}_2\text{O}_{10} \cdot 8\text{H}_2\text{O}$  generated from this solution (see Figure S12, and Tables S3 and S5 showing the structure of  $\text{K}_4\text{H}_2\text{I}_2\text{O}_{10} \cdot 8\text{H}_2\text{O}$  as previously reported).<sup>[22]</sup>

Furthermore, by using a variety of bases, such as potassium hydroxide, potassium carbonate, or potassium phosphate, in aqueous solution to adjust the pH value to 10, distinct yields of the PO-CNCs and total solids were obtained under otherwise identical conditions (Figure 2G). The yield of PO-CNCs was correlated with the alkaline strength to be on the order of  $\text{OH}^- > \text{HPO}_4^{2-} > \text{HCO}_3^-$ . It should be noted that the periodate ions were present as dimeric orthoperiodate ( $\text{H}_2\text{I}_2\text{O}_{10}^{4-}$ ) in all three solutions, independent of the base used to adjust the pH value 10 (see Figure S13). The observation of dimeric orthoperiodate ions ( $\text{H}_2\text{I}_2\text{O}_{10}^{4-}$ ) in fact differs from the findings of recent studies that showed the presence of only dianionic periodate ( $\text{H}_3\text{IO}_6^{2-}$ ) at high pH values, for example, pH 10. Although the predominance of dimeric orthoperiodate ions ( $\text{H}_2\text{I}_2\text{O}_{10}^{4-}$ ) was reported half a century ago,<sup>[23]</sup> recent studies using the sodium salt only showed evidence for dianionic periodate ions ( $\text{H}_3\text{IO}_6^{2-}$ ).<sup>[20]</sup> This difference should primarily result from the different solubilities of sodium and potassium periodate salts in aqueous solutions. At pH 10 and room temperature, the saturation concentration of potassium periodate salts in aqueous solution is approximately  $0.31 \pm 0.02 \text{ mol L}^{-1}$ , but that of sodium periodate salts is only  $0.0021 \pm 0.0003 \text{ mol L}^{-1}$ . A highly enhanced solubility of potassium periodate salts should be the reason for the formation of dimeric orthoperiodate ions ( $\text{H}_2\text{I}_2\text{O}_{10}^{4-}$ ) at pH 10.

Thus, the selective isolation of PO-CNCs from cellulose by periodate oxidation at pH 10 primarily results from the existence of dimeric orthoperiodate ions ( $\text{H}_2\text{I}_2\text{O}_{10}^{4-}$ ), which have

much lower oxidation potentials and are repulsive in the presence of PO-CNCs because of their higher negative charges (Figure 2A; see Figure S6). The structural difference between ordered and non-ordered cellulose regions promotes the selective and preferential oxidation of non-ordered parts. Hydroxide ions further degrade oxidized cellulose chains by  $\beta$ -alkoxy fragmentation into soluble small molecules and enable the isolation of PO-CNCs.

Furthermore, the reaction solutions can also be repeatedly used for the isolation of PO-CNCs from MCC for many cycles. We showcase the processes with five cycles by using  $\text{O}_3$  gas to regenerate periodate ions, primarily from iodate ions that were formed during the oxidation (Figure 3A). In particular, the alkaline conditions proved to be most beneficial for a high conversion efficiency of iodate into periodate.<sup>[24]</sup> Briefly, the supernatant transparent solutions, after the separation of the total solids, were treated with  $\text{O}_3$  gas for at least 1 hour after 14 days of reaction. Periodate was regenerated again in the solutions and enabled further isolation cycles by simply adding MCC into the solutions without any other treatment. PO-CNCs were continuously harvested at 14 days interval.

For the first five cycles, the yields of the total solids were maintained at 72 to 75 wt.%, except for the first cycle with  $56 \pm 4 \text{ wt.}\%$ . The minimal yields of PO-CNCs from cycles 2–5 were between 20–24 wt.%, and they are only slightly lower than that of the first cycle with  $27 \pm 3 \text{ wt.}\%$  (Figure 3B). As important characteristics, the size distribution and content of carboxyl groups on the surface of the PO-CNCs from the cycles 2–5 were similar to those from the first cycle. The

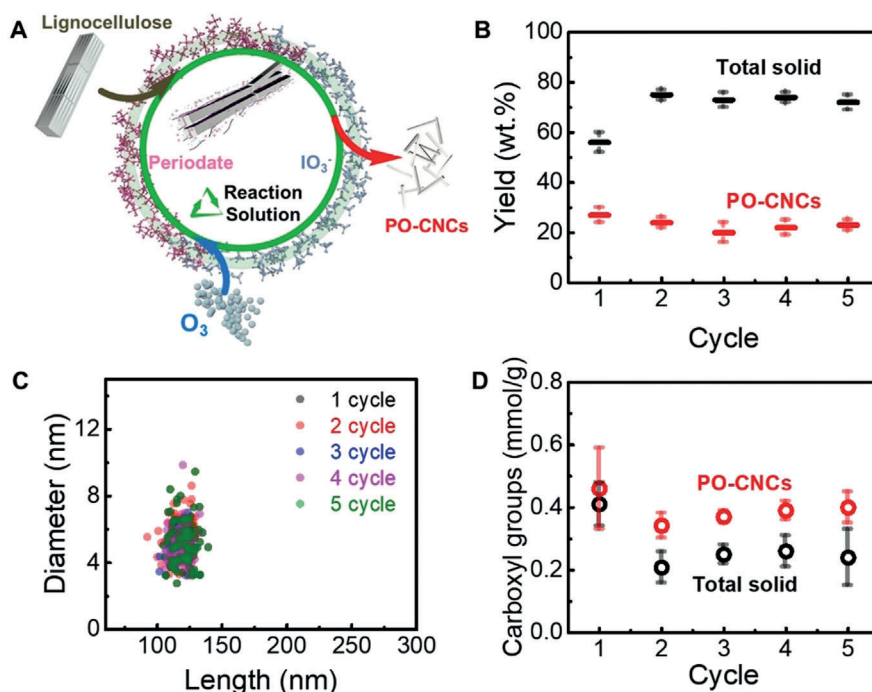


**Figure 3.** Recyclable isolation of PO-CNCs from MCC. A) Schematic representation of the recyclable isolation process by regenerating periodate with  $\text{O}_3$  gas. B) The yield of total solids and PO-CNCs from the first 5 cycles. C) Size distributions and D) The content of carboxyl groups of obtained PO-CNCs from diverse cycles.

average diameters lay between  $4.9 \pm 1.8$  and  $5.4 \pm 2.7$  nm, and the average lengths were between  $116.8 \pm 11.5$  and  $120.1 \pm 19.6$  nm. The content of the carboxy groups in the total solids was  $0.41 \pm 0.07$ ,  $0.21 \pm 0.05$ ,  $0.25 \pm 0.03$ ,  $0.26 \pm 0.05$ , and  $0.24 \pm 0.09$  mmol g<sup>-1</sup> for cycles 1–5. The content of the carboxy groups on the CNCs for cycle 1–5 was correspondingly  $0.46 \pm 0.13$ ,  $0.34 \pm 0.04$ ,  $0.37 \pm 0.02$ ,  $0.39 \pm 0.03$ , and  $0.40 \pm 0.05$  mmol g<sup>-1</sup>. Compared to the first cycle, the yields of the PO-CNCs and total solids, as well as the contents of the carboxy groups, were only slightly reduced.

The recyclable reaction solution for the isolation of PO-CNCs is attractive as it reduces the cost of consumed chemicals for the production of PO-CNCs. In particular, it presents the potential for the cost-effective large-scale production of PO-CNCs.

In addition to MCC and wood pulp containing nearly pure cellulose, various native lignocellulosic raw materials can also be directly used for isolating PO-CNCs (Figure 4). These lignocelluloses include sawdust of European beech (*Fagus sylvatica*) and Scots pine (*Pinus sylvestris*), and natural plant fibers such as flax and kenaf. PO-CNCs were facily obtained directly after selective alkaline periodate oxidation at pH 10 using the same procedure as described above for MCC (Figure 1A). The yield of the PO-CNCs from various lignocelluloses was positively correlated with the cellulose content in the corresponding raw materials (Figure 4A and B; see Table S5).  $33 \pm 2$  wt. % of PO-CNCs were obtained from wood pulp with an average diameter and length of  $4.5 \pm 0.9$  and  $85.4 \pm 10.7$  nm, respectively (Figure 4C). About  $15 \pm 2$  wt. % of the PO-CNCs was isolated from European beech, and they have an average diameter and length of  $4.4 \pm 0.7$  and  $88.6 \pm 10.0$  nm, respectively. About  $20 \pm 1$  wt. % of the PO-CNCs with an average diameter of  $4.6 \pm 1$  nm and length of  $96.9 \pm 12$  nm were obtained from Scots pine. About  $28 \pm 2$  wt. % of the PO-CNCs were obtained from flax and  $23 \pm 2$  wt. % from kenaf fibers. The size distribution of the CNCs from flax fibers is  $93.8 \pm 11.8$  nm in length and  $4.8 \pm 1.2$  nm in diameter, while PO-CNCs from the kenaf fibers have an average length of  $86.9 \pm 13.7$  nm and an average diameter of  $4.6 \pm 1.2$  nm. The average lengths and diameters of the obtained PO-CNCs are distributed over a narrow range, indicating the yield of highly homogeneous CNCs. Moreover, their sizes can be slightly

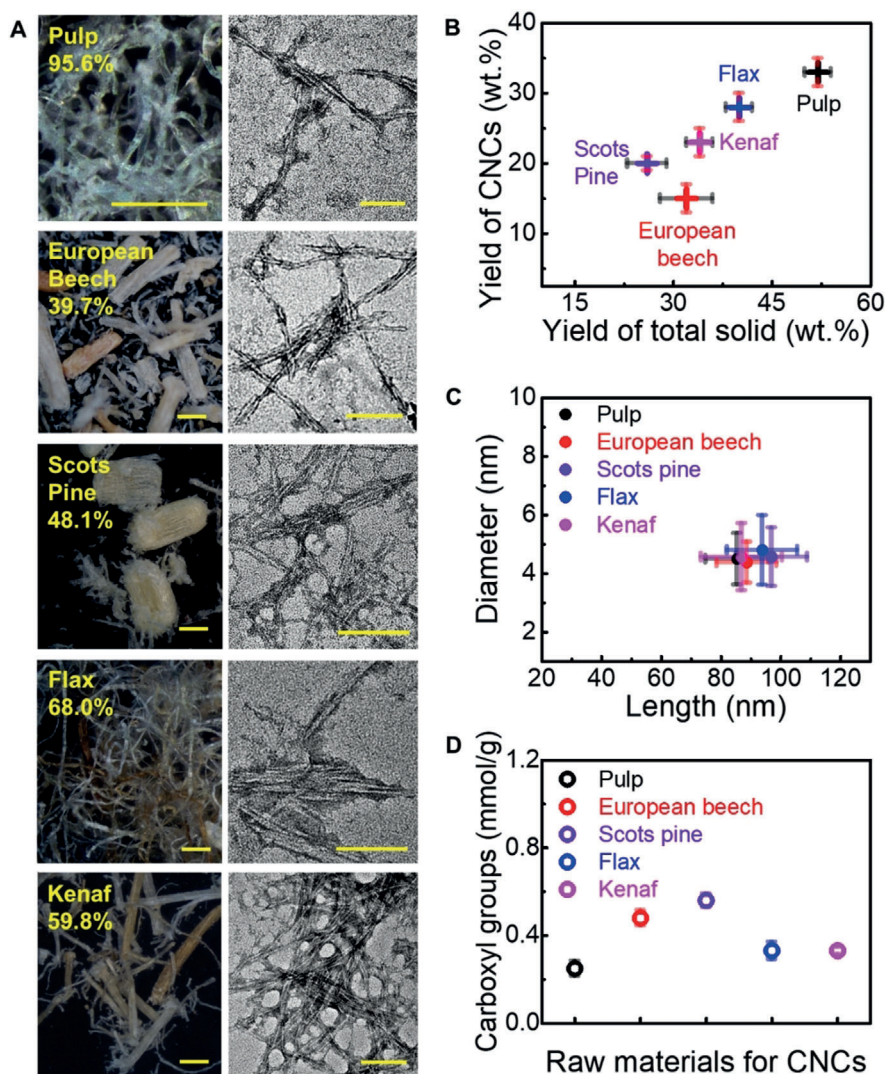


**Figure 4.** Direct isolation of PO-CNCs from various lignocelluloses. A) Microscopy images of the various starting lignocellulosic materials with the scale bars of 200  $\mu$ m and TEM images of obtained PO-CNCs with the scale bars of 100 nm. The numbers in microscopic images are cellulose contents (details in Table S5). B) Yields of total solids and PO-CNCs. C) Size distributions of obtained PO-CNCs. D) Contents of carboxy groups on PO-CNCs from various lignocelluloses.

adjusted within a small range by using distinct raw materials, but are generally smaller than CNCs from sulfuric acid hydrolysis and TEMPO-mediated oxidation.<sup>[6a]</sup> As mentioned above, these results demonstrate the selectivity of alkaline periodate oxidation of non-ordered cellulose by preferential removal of the readily hydrolysable regions down to the smallest possible dimension of the PO-CNCs. The similarity in average diameters from diverse lignocelluloses may be related to similar biosynthesis processes of cellulose in plants. Similar to PO-CNCs from MCC, the PO-CNCs from these five lignocellulosic raw materials do not contain any detectable aldehyde groups, only carboxy groups (Figure 4D). The carboxy groups were quantified by conductivity titration as follows:  $0.25 \pm 0.04$  mmol g<sup>-1</sup> for pulp CNCs,  $0.48 \pm 0.04$  mmol g<sup>-1</sup> for European beech CNCs,  $0.56 \pm 0.03$  mmol g<sup>-1</sup> for Scots pine CNCs,  $0.33 \pm 0.04$  mmol g<sup>-1</sup> for



flax CNCs, and  $0.33 \pm 0.02 \text{ mmol g}^{-1}$  for kenaf CNCs. It is worth noting here that lignin in these lignocelluloses was fragmented during the alkaline periodate oxidation and removed as soluble compounds. Thus, diverse lignocellulosic raw materials can be directly used for the isolation of CNCs by alkaline periodate oxidation at pH 10, which highly reduces the cost for the production of CNCs. In particular, complicated and time-consuming pre- and/or post-treatments using other chemicals are not required. In contrast, existing methods for the isolation of CNCs do not effectively work on such native lignocelluloses without pre- and/or post-treatments.<sup>[5,7]</sup>

## Conclusion

In summary, we showed a novel method for the efficient production of CNCs by selective alkaline periodate oxidation of ordered and non-ordered cellulose regions at pH 10. This selective periodate oxidation demonstrates a new oxidizing property of the periodate ions with diverse oxidation activities for the compounds with the same chemical composition but distinct physical structures (ordered and non-ordered). In spite of the still controversial studies regarding the types of periodate ions present in alkaline solutions,<sup>[12,20,22,25]</sup> we confirmed the presence of dimeric ortho-periodate ions ( $\text{H}_2\text{I}_2\text{O}_{10}^{4-}$ ) at pH 10 given their solubility as the potassium salt in aqueous solution.<sup>[20]</sup> Under these reaction conditions, the non-ordered cellulose regions undergo selective oxidation and subsequent  $\beta$ -alkoxy fragmentation, which are also realized for the first time within one procedure. In contrast, the oxidation of ordered regions is hampered, which leads to homogeneous PO-CNCs with very narrow distribution range of dimensions (length and diameter). Furthermore, various native lignocellulosic raw materials, including saw dusts and plant fibers, were used directly for the preparation of PO-CNCs. The surface of the PO-CNCs generally contains carboxy groups, independent of the reaction time and raw materials. Compared with the other existing methods, our method has several advantages, which include direct use of biobased raw materials (e.g., biowaste), only mild stirring at ambient conditions (i.e. intense energy input is not required), no need for pre-/post-treatments, and scalable production, even with simple equipment. This method will attract attention from both the scientific and industrial fields.

## Acknowledgements

K.Z. thanks the German Research Foundation (DFG with the project number ZH546/2-1) and the Funding for the Promotion of Young Academics of Georg-August-University of Göttingen for the financial support. P.L. and B.P. thank China Scholarship Council (CSC) for the financial support. We cordially thank Dr. Markus Euring from the Group for Chemistry and Process Engineering of Composites, University of Göttingen, for providing kenaf and flax fibers as gift. We thank Ms. Huan Liu for the AFM measurement.

## Conflict of interest

The authors declare no conflict of interest.

**Keywords:** cellulose · nanostructures · oxidation · sustainable chemistry · water chemistry

- [1] a) A. Sudalai, A. Khenkin, R. Neumann, *Org. Biomol. Chem.* **2015**, *13*, 4374–4394; b) V. V. Zhdankin, P. J. Stang, *Chem. Rev.* **2008**, *108*, 5299–5358; c) B. C. Bales, P. Brown, A. Dehestani, J. M. Mayer, *J. Am. Chem. Soc.* **2005**, *127*, 2832–2833.
- [2] a) E. L. Jackson, C. S. Hudson, *J. Am. Chem. Soc.* **1937**, *59*, 2049–2050; b) F. Brown, S. Dunstan, T. G. Halsall, E. L. Hirst, J. K. N. Jones, *Nature* **1945**, *156*, 785; c) O. A. Moe, S. E. Miller, M. H. Iwen, *J. Am. Chem. Soc.* **1947**, *69*, 2621–2625.
- [3] P. Liu, C. Mai, K. Zhang, *ACS Sustainable Chem. Eng.* **2017**, *5*, 5313–5319.
- [4] P. Liu, B. Pang, L. Tian, T. Schäfer, T. Gutmann, H. Liu, C. A. Volkert, G. Buntkowsky, K. Zhang, *ChemSusChem* **2018**, *11*, 3581–3585.
- [5] D. Klemm, E. D. Cranston, D. Fischer, M. Gama, S. A. Kedzior, D. Kralisch, F. Kramer, T. Kondo, T. Lindström, S. Nietzsche, K. Petzold-Welcke, F. Rauchfuß, *Mater. Today* **2018**, *21*, 720–748.
- [6] a) Y. Habibi, L. A. Lucia, O. J. Rojas, *Chem. Rev.* **2010**, *110*, 3479–3500; b) R. J. Moon, A. Martini, J. Nairn, J. Simonsen, J. Youngblood, *Chem. Soc. Rev.* **2011**, *40*, 3941–3994; c) N. Lin, J. Huang, A. Dufresne, *Nanoscale* **2012**, *4*, 3274–3294; d) K. J. De France, T. Hoare, E. D. Cranston, *Chem. Mater.* **2017**, *29*, 4609–4631.
- [7] E. J. Foster, R. J. Moon, U. P. Agarwal, M. J. Bortner, J. Bras, S. Camarero-Espinosa, K. J. Chan, M. J. Clift, E. D. Cranston, S. J. Eichhorn, *Chem. Soc. Rev.* **2018**, *47*, 2609–2679.
- [8] a) B. G. Rånby, *Acta Chem. Scand.* **1949**, *3*, 649–650; b) H. Bian, L. Chen, R. Gleisner, H. Dai, J. Zhu, *Green Chem.* **2017**, *19*, 3370–3379.
- [9] T. Saito, S. Kimura, Y. Nishiyama, A. Isogai, *Biomacromolecules* **2007**, *8*, 2485–2491.
- [10] J. Mao, A. Osorio-Madrado, M.-P. Laborie, *Cellulose* **2013**, *20*, 1829–1840.
- [11] a) H. Yang, D. Chen, T. G. van de Ven, *Cellulose* **2015**, *22*, 1743–1752; b) U.-J. Kim, S. Kuga, M. Wada, T. Okano, T. Kondo, *Biomacromolecules* **2000**, *1*, 488–492.
- [12] G. J. Buist, C. A. Bunton, W. C. P. Hipperson, *J. Chem. Soc. B* **1971**, 2128–2142.
- [13] A. A. Baker, W. Helbert, J. Sugiyama, M. J. Miles, *Biophys. J.* **2000**, *79*, 1139–1145.
- [14] G. Dryhurst, *Periodate oxidation of diol and other functional groups: analytical and structural applications, Vol. 2*, Elsevier, Amsterdam, **2015**.
- [15] G. Buist, C. Bunton, J. Lomas, *J. Chem. Soc. B* **1966**, 1099–1105.
- [16] I. Pavasars, J. Hagberg, H. Borén, B. Allard, *J. Polym. Environ.* **2003**, *11*, 39–47.
- [17] P. Calvini, A. Gorassini, G. Luciano, E. Franceschi, *Vib. Spectrosc.* **2006**, *40*, 177–183.
- [18] H. Yang, T. G. M. van de Ven, *Cellulose* **2016**, *23*, 1791–1801.
- [19] J. Leguy, A. Diallo, J.-L. Putaux, Y. Nishiyama, L. Heux, B. Jean, *Langmuir* **2018**, *34*, 11066–11075.
- [20] L. Valkai, G. Peintler, A. K. Horváth, *Inorg. Chem.* **2017**, *56*, 11417–11425.
- [21] a) J. Aveston, *J. Chem. Soc. A* **1969**, 273–275; b) G. J. Buist, W. C. P. Hipperson, J. D. Lewis, *J. Chem. Soc. A* **1969**, 307–312.



- [22] A. Ferrari, A. Braibanti, A. Tiripicchio, *Acta Crystallogr.* **1965**, *19*, 629–636.
- [23] G. J. Buist, J. D. Lewis, *Chem. Commun.* **1965**, 66–67.
- [24] S. Koprivica, M. Siller, T. Hosoya, W. Roggenstein, T. Rosenau, A. Potthast, *ChemSusChem* **2016**, *9*, 825–833.
- [25] J. E. Taylor, *J. Phys. Org. Chem.* **2007**, *20*, 1088–1092.

Manuscript received: September 20, 2019

Revised manuscript received: October 29, 2019

Accepted manuscript online: November 6, 2019






Version of record online: ■ ■ ■ ■, ■ ■ ■ ■



## Research Articles



## Sustainable Chemistry

P. Liu, B. Pang, S. Dechert, X. C. Zhang,  
L. B. Andreas, S. Fischer, F. Meyer,  
K. Zhang\*     

Structure Selectivity of Alkaline Periodate Oxidation on Lignocellulose for Facile Isolation of Cellulose Nanocrystals



**Structure based:** A novel method based on a recyclable and newly selective alkaline periodate oxidation at pH 10 provides a sustainable strategy for the efficient isolation of cellulose nanocrystals (CNCs) from various lignocellulosic materials. The isolation of the CNCs results from the structural differences between the ordered and non-ordered regions of the lignocellulose.